Wang *et al. Nanoscale Research Letters* (2018) 13:78
https://doi.org/10.1186/s11671-018-2486-5

Nanoscale Research Letters

NANO EXPRESS Open Access

Facile Synthesis of Ultralong and Thin Copper Nanowires and Its Application to High-Performance Flexible Transparent Conductive Electrodes

Yaxiong Wang[1,2], Ping Liu[1,2*], Baoqing Zeng[1], Liming Liu[2] and Jianjun Yang[2]

Abstract

A hydrothermal method for synthesizing ultralong and thin copper nanowires (CuNWs) with average diameter of 35 nm and average length of 100 μm is demonstrated in this paper. The concerning raw materials include copric (II) chloride dihydrate ($CuCl_2 \cdot 2H_2O$), octadecylamine (ODA), and ascorbic acid, which are all very cheap and nontoxic. The effect of different reaction time and different molar ratios to the reaction products were researched. The CuNWs prepared by the hydrothermal method were applied to fabricate CuNW transparent conductive electrode (TCE), which exhibited excellent conductivity-transmittance performance with low sheet resistance of 26.23 $\Omega/\square$ and high transparency at 550 nm of 89.06% (excluding Polyethylene terephthalate (PET) substrate). The electrode fabrication process was carried out at room temperature, and there was no need for post-treatment. In order to decrease roughness and protect CuNW TCEs against being oxidized, we fabricated CuNW/poly(methyl methacrylate) (PMMA) hybrid TCEs (HTCEs) using PMMA solution. The CuNW/PMMA HTCEs exhibited low surface roughness and chemical stability as compared with CuNW TCEs.

Keywords: Copper nanowire, Transparent conductive electrode, Hydrothermal synthesis

Background

Transparent conductive electrodes (TCEs) are extremely important parts in many optoelectronic devices including organic light-emitting diodes (OLEDs), solar cells, liquid crystal displays, Flat-panel displays, sensors and so on [1–7]. Indium tin oxide (ITO) is one of the most commonly used TCEs in industry, which possesses low resistivity ($\sim 10 - 30\Omega/\square$) at high optical transparency (90%) [8]. It is a great pity that indium is a rare metallic element and its' abundance in the earth's crust is very low, which leads to the price of ITO becoming more and more expensive [8–10].

Hence, researchers have done a lot of attempts to develop some new materials to partially replace ITO. These candidates should possess low cost, high conductivity, high transmittancy, and excellent flexibility and can be deposited at low temperatures. Among those candidates, metallic nanowires are especially promising. Recent studies have reported the use of silver nanowires (AgNWs); transparent electrodes based on AgNWs have been reported to compete well with ITO [11–19]. However, silver is a precious metal, and its expensive price should not be ignored. As a result of the increasing demand for low-cost metallic nanowires, copper has received considerable attention as an interesting alternative to silver. Copper is almost as conductive as silver, because bulk resistivity of copper is 1.67 $n\Omega \cdot m$, while that of silver is $1.59 n\Omega \cdot m$ [20]. Moreover, copper is much more abundant and far less expensive than silver and ITO. Based on these facts, more and more attention is paid to copper nanowires (CuNWs).

Thus, various methods for preparing CuNWs have been studied, such as chemical vapor deposition,

*Correspondence: liuping49@uestc.edu.cn
[1]School of Physical Electronics, University of Electronic Science and Technology of China, Chengdu 610054, China
[2]College of Electron and Information Engineering, University of Electronic Science and Technology of China Zhongshan Institute, Zhongshan 528402, China

electrochemical deposition, template, and membrane processes [21–26]. However, these methods involve several complex processes and require toxic chemical reagents or valuable catalyst. Probably, hydrothermal methods seem to be one simple way for the production of CuNWs. Zhang et al. prepared CuNWs (or copper nanorods) with diameter being about 50 nm and length reaching up to $> 10\ \mu$m by means of hydrothermal synthesis with ascorbic acid as reducing agent and polyvinyl pyrrolidone (PVP) as capping agent at relatively low temperature [27]. Wang et al. prepared ultralong CuNWs with a uniform diameter of about 800–1000 nm and a typical length of several tens of micrometers by applying ascorbic acid as reductant and capping agent [28]. Using octadecylamine (ODA) as both a soft reducing agent and an adsorption agent, Shi et al. obtained ultralong CuNWs with length up to several millimeters and diameters of 30–100 nm [29]. Melinda Mohl and co-workers applied the copper chloride and glucose in the presence of hexadecylamine (HDA), successfully prepared some long CuNWs with a uniform diameter of 64 ± 8 nm and length of a few micrometers [30]. Aziz et al. elaborated a simple hydrothermal method to produce CuNWs with length of twenties micrometers by using HDA and potassium bromide as capping agent [31]. Kim et al. reported a seed-mediated synthetic strategy for CuNW production, and some typical scanning electron microscopy (SEM) images on CuNWs showed that average diameter was 21.9 ± 3.8 nm, and the maximum length was 77.1 μm [32].

Compared with CuNWs, fabrication on CuNW TCEs has been scarcely studied, since instability and the feature of being easily oxidized often lead to CuNW films to be non conductive. Wiley and coworkers have achieved good results in the preparation of CuNWs and CuNW TCEs. In 2010, it was the first time that they had prepared CuNW TCEs on flexible substrate with a sheet resistance of 30 $\Omega/\square$ at specular transmittance of 85% by means of Meyer rod coating [33]. In 2014, They improved the way to produce CuNWs and then made CuNW TCEs with a transmittance > 95% at a sheet resistance < 100 $\Omega/\square$ [34]. Simonato's group treated CuNWs with glacial acetic acid to fabricate flexible CuNW TCEs exhibiting a sheet resistance of 55 $\Omega/\square$ at 94% transmittance (λ=550 nm) by means of vacuum filtration [20]. Chu et al. prepared CuNW TCEs with 52.7 $\Omega/\square$ at T=90% (λ=400–700 nm) using a spray coating, which were not conductive before annealing in a furnace for 2 h in an atmosphere of 75% argon and 25% hydrogen [35]. However, despite these efforts, CuNW-based TCEs still present a number of limitations that prevent their widespread use. One problem is their high surface roughness when deposited on bare substrates and another problem is that CuNWs have low oxidation potential and chemical stability.

One way to improve the performance of nanowire films is to use nanowires with higher aspect ratios [34]. Short and coarse CuNWs are not suitable for the preparation of TCEs. For example, CuNWs with diameters about 50 nm and length about 10 μm proposed in Ref. [27] are too short to prepare high-quality TCEs. It is worth noting that too long CuNWs are also not suitable for the preparation of TCEs, because it is too easy for them to get together and can not be well-dispersed. For example, length of CuNWs proposed in [29] was up to several millimeters, and many of CuNWs bundle together [29]. Moderate lengths and diameters of CuNWs are very important for high-quality CuNW TCEs. In this paper, a simple hydrothermal approach for the synthesis of thin, well-dispersed, and ultralong CuNWs with average diameter of 35 nm and average length of 100 μm is reported, where ODA, ascorbic acid, and copric (II) chloride dihydrate ($CuCl_2 \cdot 2H_2O$) are involved. $CuCl_2 \cdot 2H_2O$ provides copper source, ascorbic acid is used as reducing agent, and ODA is selected as capping agent. The lengths and diameters of CuNWs are affected by the reaction time, molar ratio of the three drugs, and we will reveal the effects of these factors. The ultralong and thin CuNWs were used to fabricate CuNW TCEs at room temperature. The sheet resistance of the CuNW TCE was as low as 26.23 $\Omega/\square$ at 89.06% transmittance (λ=550 nm). In order to reduce roughness of CuNW TCEs and prevent CuNWs from being oxidized, poly(methyl methacrylate) (PMMA) was coated on surface of CuNW TCEs to prepare CuNW/PMMA hybrid TCEs (HTCEs), and the effects of PMMA on transmittance and roughness of CuNW TCEs are demonstrated.

Experimental

Synthesis of CuNWs

In a typical process for synthesizing CuNWs, 140-mg ascorbic acid ($C_6H_8O_6$, Aladdin) and 270-mg $CuCl_2 \cdot 2H_2O$ (Aladdin) were added to 282 ml of ODA (26.3 mmol L^{-1}) aqueous solution. Molar concentrations of ascorbic acid and $CuCl_2 \cdot 2H_2O$ are 2.8 mmol L^{-1} and 5.6 mmol L^{-1}, respectively. The mixed solution turned to homogeneous suspension after 60 min of normal temperature sealing stirring. Subsequently, the obtained suspension was transferred into a Teflon-lined autoclave and sealed for 20 h at 120 °C. The reactor was then cooled down to room temperature naturally. The excess chemicals were removed by washing with deionized water and ethanol. The final product was kept in 130-ml glacial acetic acid (Aladdin) to avoid oxidation of CuNWs.

Fabrication of CuNW TCEs and CuNW/PMMA HTCEs

CuNW TCEs were fabricated on Polyethylene terephthalate (PET) substrates (188 μm thickness). A slight amount of glacial acetic acid solution containing CuNWs was diluted by 500-ml deionized water. TCEs were formed at

room temperature by filtration of a dispersion of CuNWs on a mixed cellulose ester (MCE) filter membrane (0.45 μm). The deposited film was then transferred to the PET substrate by applying uniform pressure. The MCE filter membrane was peeled off to keep the CuNW network on the PET substrate. 100 ul PMMA solution(20 mg/ml) was coated onto surface of CuNW TCEs using a spin coater at 800 rpm for 5 s and 2500 rpm for 30 s. CuNW/PMMA HTCEs were naturally dried without thermal sintering.

Structural, Optical, and Electrical Characterization

The morphology and dimensions of the synthesized CuNWs were investigated by SEM (JSM-7500F, JEOL) and transmission electron microscopy (TEM) (FEI-TECNAL G20) . Surface morphology images of the CuNWs were analyzed by an optical microscope (BX51M, OLYMPUS). The transmittances of CuNW TCE and CuNW/PMMA HTCE were determined by a UV spectrophotometer (GZ502A, Shanghai shine Photoelectric Technology Co., Ltd.). Roughness of CuNW TCEs and CuNW/PMMA HTCEs was determined by an atomic force microscope (AFM) (Dimension Edge, BRUKER). The powder X-ray diffraction (XRD) patterns of CuNWs were performed by XRD analysis (Bruker, BRUKER OPTICS).

Two sheets of aluminum (Al) film were deposited at both ends of a CuNW/PMMA HTCE or a CuNW TCE, as shown in Fig. 1. The distance between the two inner sides of the aluminum films is marked as length L, and the distance between the other two sides of the TCE is marked as width W. Relationship of resistance R of a film and its sheet resistance R_s is constrainted by the formula as follows [36]:

$$R_s = R\frac{W}{L} \tag{1}$$

Resistance of CuNW TCE and CuNW/PMMA HTCE was measured by a multimeter and the sheet corresponding resistances were concluded from the resistances with the help of Formula (1). For example, the resistance of a CuNW/PMMA HTCE is 65.9 Ω, as shown in Fig. 1, L is 19.2 mm and W is 27.6 mm, respectively. Then, one can conclude that the sheet resistance of the CuNW/PMMA HTCE in Fig. 1 is 94.7 Ω/□.

Results and Discussion

Synthesis of CuNWs

In this work, well-dispersed CuNWs with an average diameter of 35 nm, an average length of 100 μm, and aspect ratio about 2857 were synthesized by the reduction of $CuCl_2 \cdot 2H_2O$ with ascorbic acid through a hydrothermal reduction process. ODA acted as capping agent in the process of the growth of CuNWs. The three materials are all very cheap, so the cost of preparing CuNWs is very low. Different reaction time and different molar ratios will lead to different products, and we will discuss these factors in the following subsections.

(A) Characterization of CuNWs

The CuNWs were prepared by the method in the "Synthesis of CuNWs" subsection of the "Experimental" section. The photograph of CuNWs obtained is shown in Fig. 2a. The morphology and dimension of the corresponding CuNWs are shown by SEM in Fig. 2b, c. It is shown in Fig. 2b, c that the final product is composed of a large quantity of CuNWs with average diameter of 35 nm and average length of 100 μm, thus featuring an aspect ratio about 2857. Long NWs with a high aspect ratio are required in order to achieve high electrical conductivity and transmittance in the NWs-based web structures,

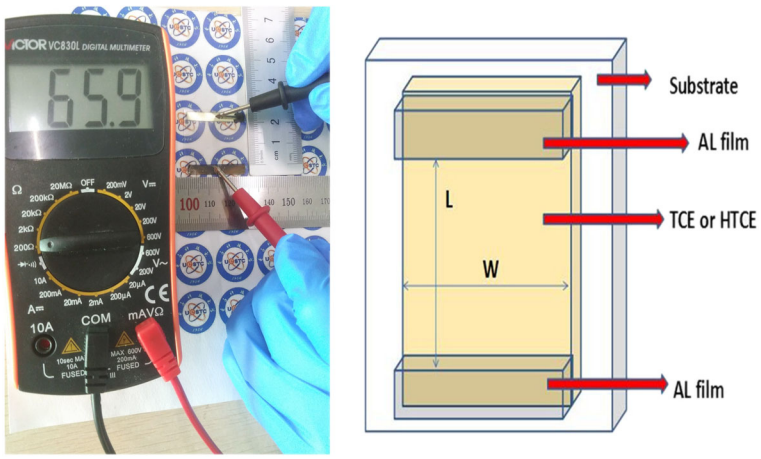

Fig. 1 Photographic image and schematic illustration testing resistance process. Left is photographic image of testing resistance process, and right shows schematic illustration of length and width of a TCE

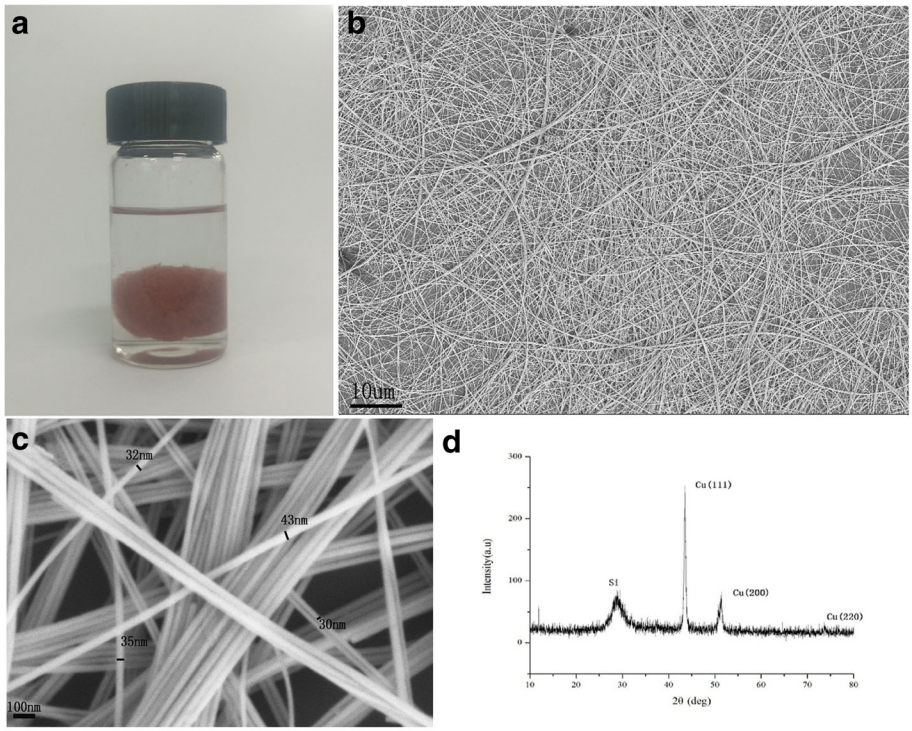

Fig. 2 Structure of CuNWs. **a** The CuNWs as-prepared in acetate. **b** SEM image of CuNWs from a general view. **c** SEM image of CuNWs from a detailed view. **d** Powder XRD pattern of the CuNWs drop-casted on a silicon substrate

because they enable fully inter-networked, highly conductive pathways even with low nanowire density [37, 38]. Consequently, the method mentioned above is applicable for the production of uniform CuNWs. These thin and uniform CuNWs make it possible to prepare high-performance CuNW TCEs. Figure 2d depicts the XRD pattern of CuNWs drop-casted on a silicon substrate. CuNWs are identified on the basis of the three distinguishable diffraction peaks at 43.316, 50.448, and 74.124, corresponding to {1 1 1}, {2 0 0}, and {2 2 0} crystal planes of face-centered cubic copper, respectively. The intensity of {1 1 1} crystal planes of face-centered cubic copper higher than those of the others indicates the enrichment of {1 1 1} crystal planes of the CuNWs. The result also

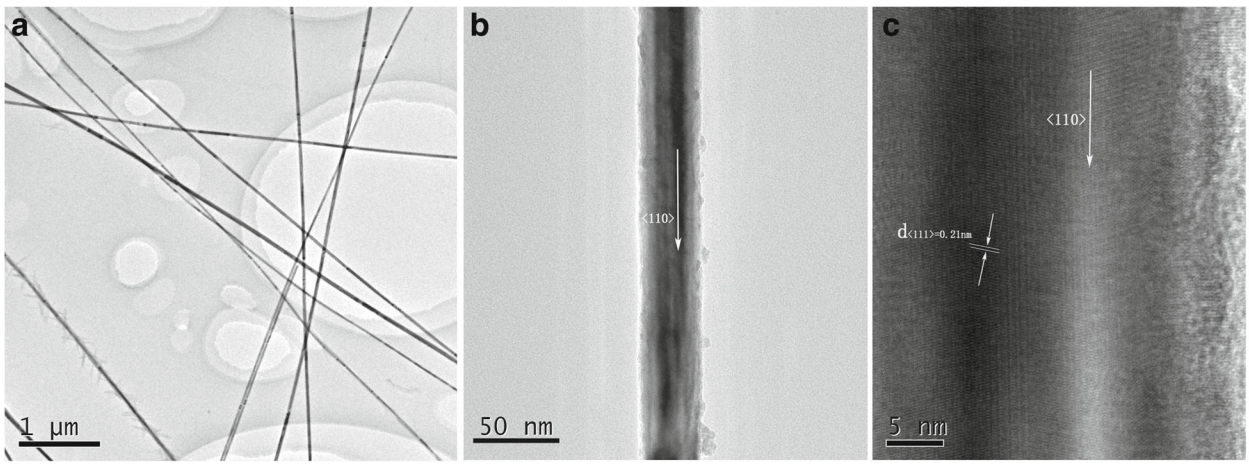

Fig. 3 TEM images and HRTEM image of CuNWs. **a**, **b** TEM images of CuNWs. **c** HRTEM image of a CuNW. The lattice spacing was observed to be 0.21 nm

indicates that copper atoms firstly deposited on {1 1 1} facets, led to one-dimensional (1-D) CuNWs. No signal from impurities such as CuO and Cu_2O was observed in the XRD pattern, which indicates pure CuNWs were obtained.

Figure 3a, b shows TEM images of ultra-long CuNWs with diameters about 35 nm. We can observe that the surfaces of the copper nanowires are very smooth. Figure 3c proposes high-resolution TEM (HRTEM) image of a CuNW. The lattice spacing was observed to be 0.21 nm, which corresponds to the {1 1 1} plane of face center cubic copper.

(B) Time-Dependent Analysis

In order to observe the growth process of the CuNWs, the products were investigated by SEM. Products obtained after 1- to 40-h hydrothermal treatment at 120 °C exhibited different morphologies and length. Morphology of CuNWs with different reaction time are studied by SEM. SEM images of samples at different stages of hydrothermal treatment are shown in Fig. 4.

From Fig. 4a, one can see that the product is mostly composed of copper nanocubes and almost no CuNWs is produced when the reaction time is 1 h, which indicates an isotropic growth dominated system. The reason is that the

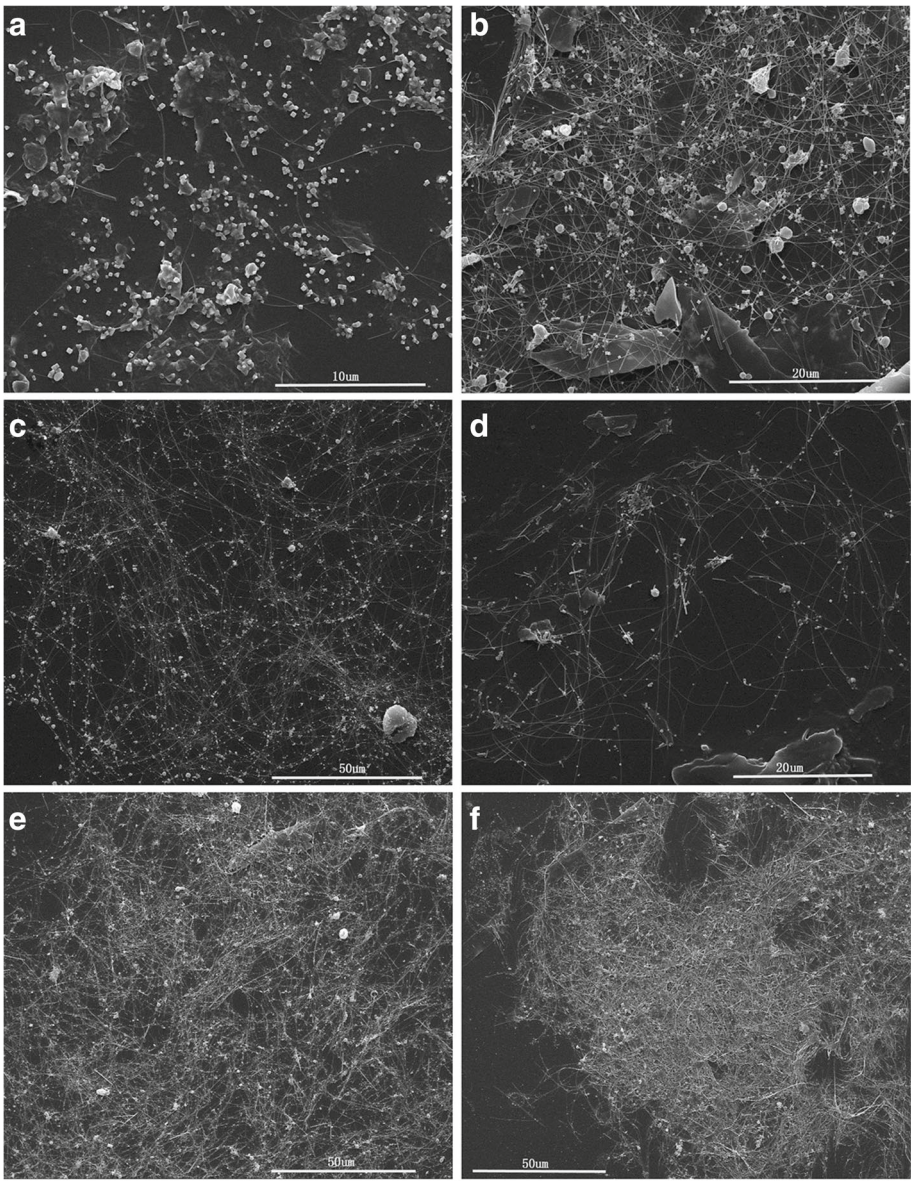

Fig. 4 SEM images of samples at different reaction time of hydrothermal treatment. The different reaction time of hydrothermal treatment are **a** 1 h, **b** 2 h, **c** 6 h, **d** 14 h, **e** 20 h, and **f** 40 h

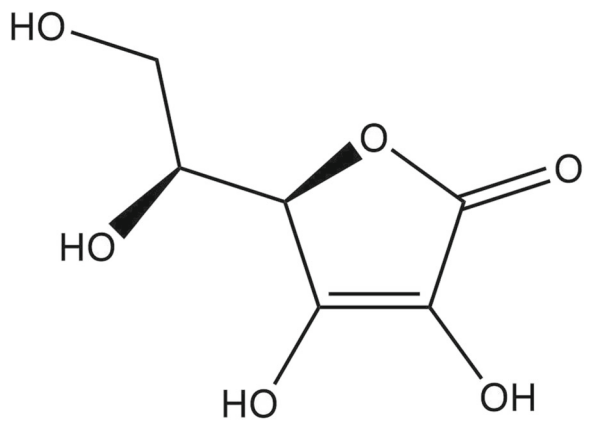

Fig. 5 Chemical structural formula of ascorbic acid. There are four hydroxyls (-OH) in one ascorbic acid molecule, which act as the functional group in this reduction reaction

capping agent was insufficient to cover all newly formed {1 0 0} facets on copper nanocrystals in this stage. Since the growth mechanism of CuNWs is not yet fully understood, so we speculate that only a small fraction of the ODA is vaporized and dissolved under high pressure at the initial stage. Therefore, there is no enough capping agent to ensure the anisotropic growth of the crystal.

As time goes on, more and more ODA are gasified to produce sufficient capping agents, and then 1D growth on these nanocrystal seeds in aqueous leads to the formation of CuNWs. As shown in Fig. 4b–d, more and more raw materials turn to products and more and more nanocrystal seeds convert into CuNWs when time goes from 2 to 14 h. Meanwhile, we can see that the lengths of the CuNWs are becoming longer and longer in the range of 2 to 14 h, and the average length of CuNWs is about 25, 60, and 80 μm in Fig. 4b–d, respectively. The CuNWs are very thin and their average diameter is only about 35 nm. When the CuNWs are longer than 100 μm, they become to be easily broken, so their lengths no longer increase. Figure 4e, f indicates that the lengths and diameters of the CuNWs do not change significantly within 20 to 40 h.

(C) Amount of Ascorbic Acid

Ascorbic acid was selected as reducing agent in the synthesis of CuNWs. To investigate the influence of the amount of ascorbic acid on the morphology of the CuNWs, the amounts of deionized water, ODA, and $CuCl_2 \cdot 2H_2O$ were fixed and the amount of ascorbic acid was changed. After 20 h of heating in a sealed Teflon-lined autoclave at 120 °C, the obtained solution was washed with deionized water and ethanol. The final products were observed with the help of an optical microscope.

Chemical structural formula of ascorbic acid can be written as shown in Fig. 5. There are four hydroxyls (-OH) in one ascorbic acid molecule, which act as the functional group in this reduction reaction, and there is one Cu^{2+}

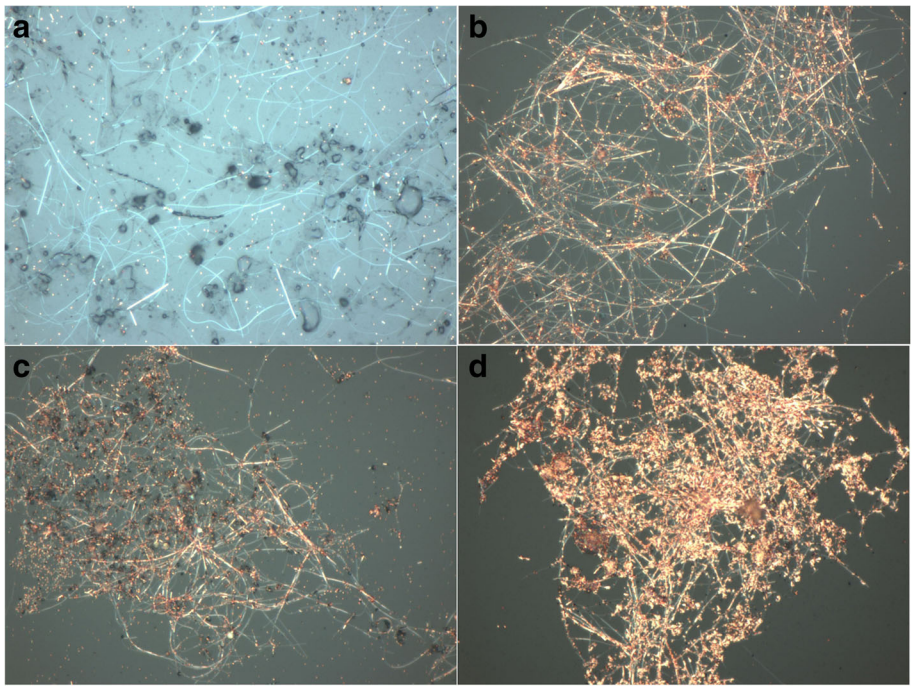

Fig. 6 Optical microscope images of CuNWs synthesized with different molar ratios of ascorbic acid and $CuCl_2 \cdot 2H_2O$. The different molar ratios of ascorbic acid and $CuCl_2 \cdot 2H_2O$ are **a** 0.2 : 1, **b** 0.5 : 1, **c** 1 : 1 and **d** 2 : 1

Table 1 Transmittances (excluding PET substrate) at 550 nm and sheet resistances of CuNW TCEs

Sample	A	B	C	D	E
R_s (Ω/□)	87.21	62.51	26.23	24.15	16.68
Transmittance	92.53%	90.77%	89.06%	81.46%	77.84%

in one $CuCl_2 \cdot 2H_2O$ molecule, so one can assume that optimum molar ratio of ascorbic acid and $CuCl_2 \cdot 2H_2O$ is 0.5 : 1. Figure 6 demonstrates the optical microscope images of the final products with different molar ratios of ascorbic acid and $CuCl_2 \cdot 2H_2O$. When the molar ratio is 0.5 : 1, the largest amount of CuNWs is produced (Fig. 6b) and the amount of copper nanoparticles (CuNPs) is relatively much smaller. Upon increasing the molar ratio to 1 : 1 or 2 : 1, more and more CuNPs appear in the optical microscope images (Fig. 6c, d). At the molar ratio of 2 : 1, the product contains a large number of CuNPs and any CuNWs are hardly formed. This is probably because that CuNWs grow from multi-twinned seeds. However, multi-twinned seeds are unstable at initial stages if their {1 0 0} facets are not well capped. the crystal growth on the {1 0 0} facets could rapidly develop multi-twinned seeds into single-crystal seeds, which only produce CuNPs. When the molar ratio of reducing agent is much larger than the appropriate value, a large number of multi-twinned seeds will appear at the beginning stage. At the same time, the ODA is not heavily vaporized, and diffusing in the aqueous, resulting in the lack of capping agent. In the case of the ratio is 0.2 : 1 in Fig. 6a, the solution is very viscous and contain a large amount of ODA, which makes it very difficult to separate the CuNWs from the solution. Small amounts of CuNPs and CuNWs are produced in Fig. 6a, and we can assume that in this case only part of copper are reduced since the amount of reducing agent is less than normal.

Fabrication of CuNW TCE

The vacuum filtration transfer method is a simple and scalable method to make TCEs. By means of vacuum filtration transfer, the solutions containing NWs can be adequately diluted and be dispered as individual wires, so the prepared TCEs possess good conductivity. Meanwhile, some reagent can be filtered out, which is helpful to improve electrical conductivity of the TCEs. In this work, the glacial acetic acid solution containing CuNWs is diluted by deionized water and then filtered on a MCE filter membrane. During the process, the residual organic materials and copper oxides can be removed, which helps to improve electrical conductivity of the CuNW TCEs.

The transmittance of a TCE depends on the amount of CuNWs deposited on the substrates, and it will drastically decrease when the sheet resistance of the TCE decreases. High conductivity and high transmittancy of the CuNW TCEs are mainly attributed to the morphology of CuNWs such as long length, small diameter, absence of NPs and any other residual organic matters [39–41]. In this work, we select the reaction time as 20 h and molar ratio of ascorbic acid and $CuCl_2 \cdot 2H_2O$ as 0.5 : 1. Table 1 lists sheet resistances and transmittances (excluding PET substrate)

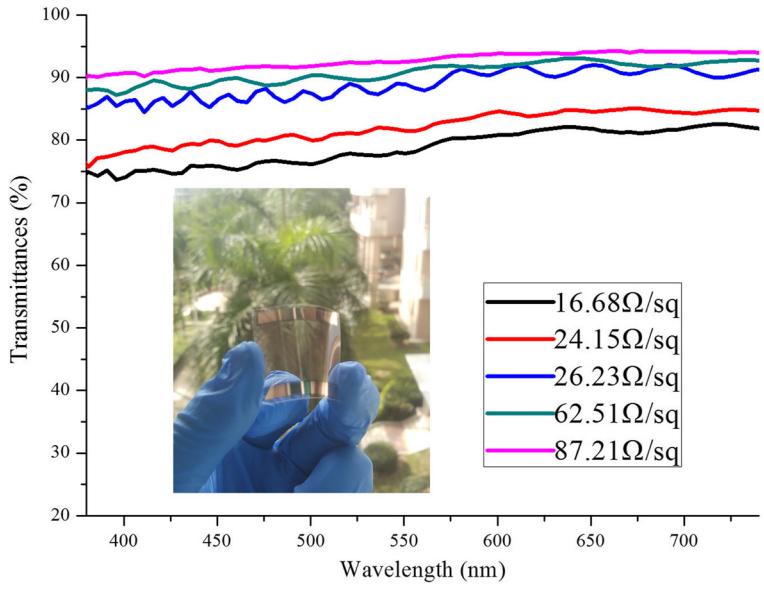

Fig. 7 Transmittance spectra (366–741 nm) of the CuNW TCEs with various sheet resistances. Sheet resistances and transmittance of the five samples at 550 nm are listed in Table 1. Photographic image of a CuNW TCE is demonstrated, whose transmittance at 550 nm is 89.06% on condition that effect of PET is excluded

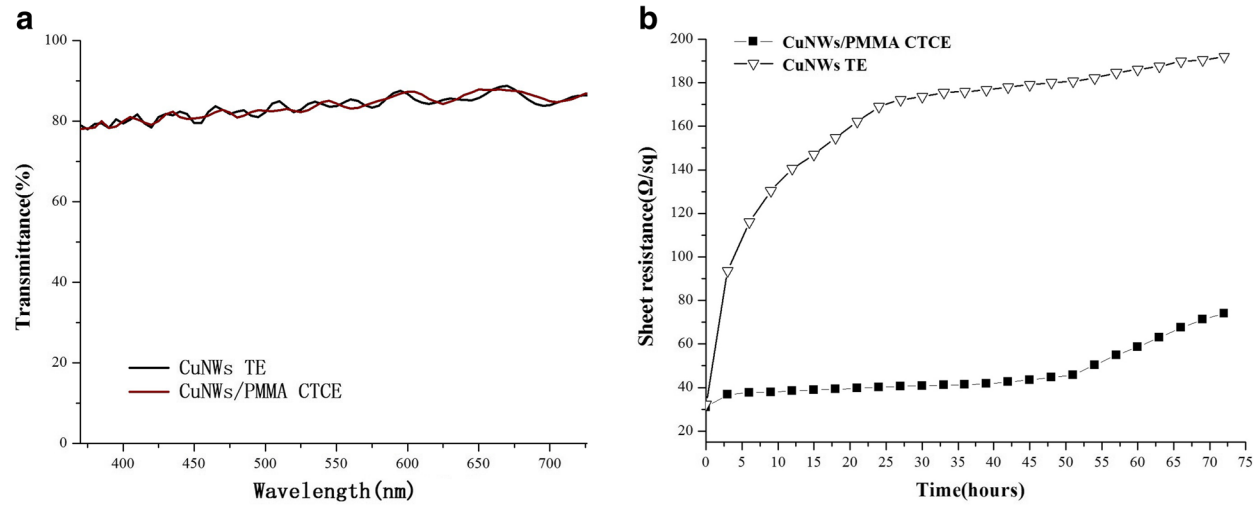

Fig. 8 Optoelectronic properties comparison of a CuNW TCE and a CuNW/PMMA HTCE. **a** CuNW TCE and CuNW/PMMA HTCE possess similar transmittance spectra. **b** The change in the sheet resistance of CuNW and CuNW/PMMA HTCEs stored under ambient conditions for 72 h

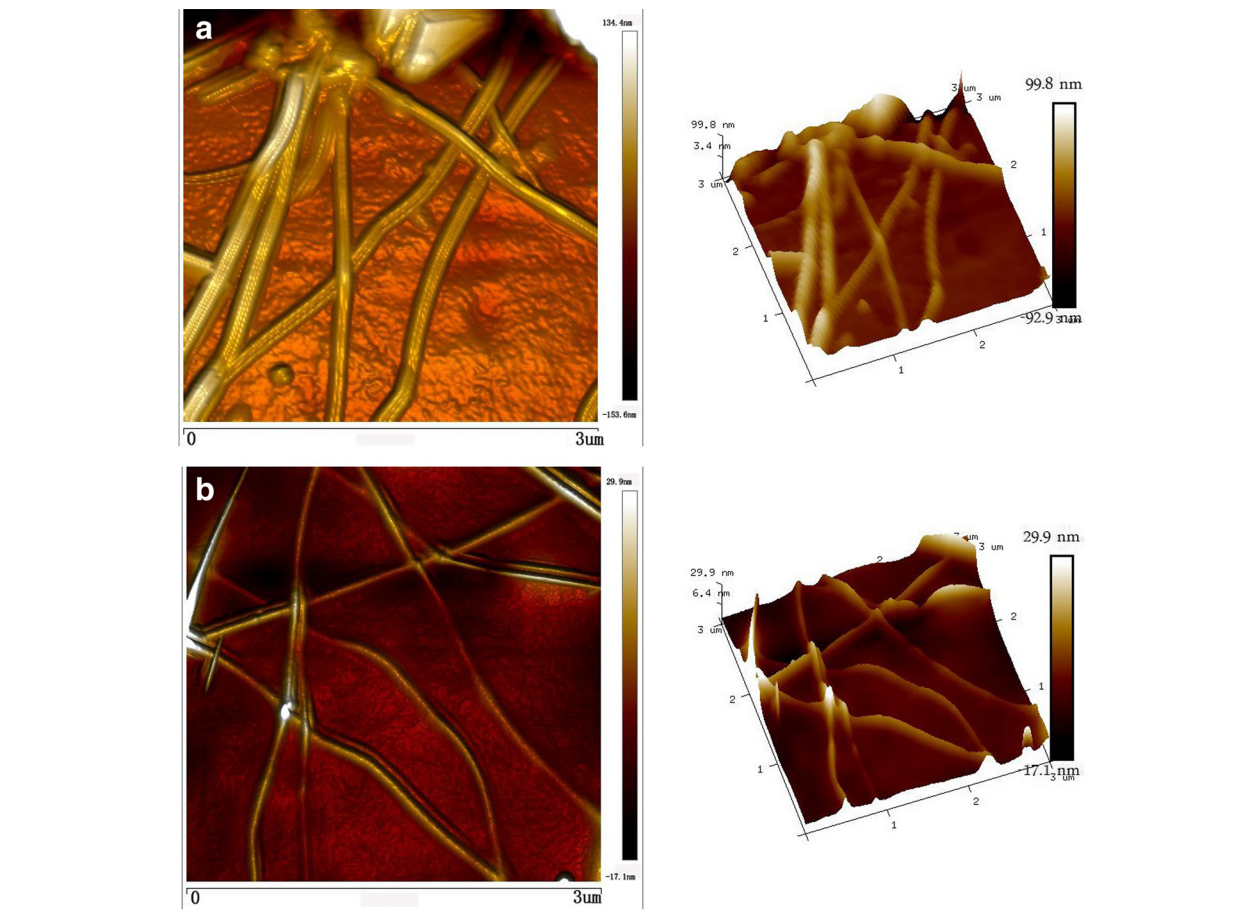

Fig. 9 AFM topographic images of **a** CuNW TCE and **b** CuNW/PMMA HTCE. The left images are original AFM images, and the right images show the RMS surface roughness

at 550 nm for five CuNW TCEs. The fact that higher transmittances are related to lower sheet resistances is in line with the existing observations. Transmittances at wider range (λ=366–741 nm) for the five samples are proposed in Fig. 7. The photographic image of sample C is also demonstrated in Fig. 7, whose transmittances is 89.06% at 550 nm (excluding PET substrate).

Fabrication of CuNW/PMMA HTCE

Although CuNW TCEs have many advantages, some fatal shortcomings cannot be ignored, including high roughness and low chemical stability, which limit their applications. In order to overcome these problems, we fabricated CuNW/PMMA HTCEs by spin coating PMMA solution 20 mg/ml to reduce the roughness and prevent the CuNWs oxidation. The properties of the CuNW TCEs and CuNW/PMMA HTCEs were compared. Figure 8a, b shows transmittance graphs and the changes in conductivity of a CuNW TCE and a CuNW/PMMA HTCE on a PET substrate, respectively. Figure 8a shows that the CuNW TCE and the CuNW/PMMA HTCE possess similar transmittance spectra. From Fig. 8b, we can see that sheet resistances of the CuNW TCE and the CuNW/PMMA HTCE were also similar to each other when they have just been prepared. Sheet resistance of the CuNW TCE increased rapidly from 32.1 Ω/□ to 93.5 Ω/□ after 3 h. However, sheet resistance of CuNW/PMMA HTCE showed a slow increase, which was almost unchanged when 50 h passed and remained still very low (74 Ω/□) when 72 h passed. The stability was significantly improved after the CuNW TCE was coating with PMMA to form a CuNW/PMMA HTCE. Thus, the PMMA coating effectively protected the CuNWs from moisture and oxygen.

As mentioned above, large roughness is not compatible with various applications and can cause short circuits in electronic devices. Therefore, smooth surfaces are crucial to the practical application of the optoelectronic devices. We embedded CuNWs in the PMMA film to reduce roughness. Figure 9 demonstrates AFM topographic images of a CuNW TCE and a CuNW/PMMA HTCE. In Fig. 9a, the surface topography of the CuNW TCE is relatively rough, whose root-mean-square (RMS) surface roughness is 31.2 nm. In Fig. 9b, the surface topography of the CuNW/PMMA HTCE appears very smooth, whose RMS surface roughness is 4.8 nm. It is obvious that the spin coated PMMA film can greatly reduce surface roughness of the CuNW film because the PMMA solution can fill holes between the random grids of CuNWs.

Conclusions

A hydrothermal method for synthesizing ultralong and thin CuNWs is proposed in this paper. The average diameter of the CuNWs is about 35 nm, and the average length is about 100 μm, and the corresponding aspect ratio is about 2857. The concerning raw materials include $CuCl_2 \cdot 2H_2O$, ODA and ascorbic acid, which are all very cheap and nontoxic. In the hydrothermal process, $CuCl_2 \cdot 2H_2O$ provides copper source, ascorbic acid acts as the reducing agent, and ODA was used as the capping agent.

CuNW TCEs were fabricated by CuNWs prepared by the hydrothermal method. The best result we achieved for the CuNW TCEs was $R_s = 26.23$ Ω/□ for T= 89.06% at 550 nm (excluding PET substrate). The TCE fabrication process was carried out at room temperature, and there was no need for post-treatment such as thermal annealing and opto-thermal heating. To reduce roughness and prevent against oxidation of CuNW TCEs, we fabricated CuNW/PMMA HTCEs. The experiments showed that CuNW/PMMA HTCE possessing lower roughness and higher antioxidant activity compared to CuNW TCE.

Abbreviations

AFM: Atomic force microscope; AgNWs: Silver nanowires; CuNPs: Copper nanoparticles; CuNWs: Copper nanowires; HDA: Hexadecylamine; HRTEM: High resolution transmission electron microscopy; HTCE: Hybrid transparent conductive electrode; HTCEs: Hybrid transparent conductive electrodes; ITO: Indium Tin Oxide; MCE: Mixed cellulose ester; ODA: Octadecylamine; OLEDs: Organic light-emitting diodes; PET: Polyethylene terephthalate; PMMA: Poly(methyl methacrylate); PVP: Polyvinyl pyrrolidone; RMS: Root-mean-square; TCE: Transparent conductive electrode; TCEs: Transparent conductive electrodes; TEM: Transmission electron microscopy; XRD: X-ray diffraction

Acknowledgements

The authors would like to thank Professor Yue-Hui Wang for her valuable discussion.

Funding

The work was supported by the National Natural Science Foundation of China (Nos. 61571103 and 11775047) and the Science and Technology Project Foundation of Zhongshan (No. 2017B1016).

Availability of Data and Materials

The datasets supporting the conclusions of this article are included within the article.

Authors' Contributions

YW did the most experiments in this work, YW and PL drafted the manuscript, BZ made the research plan, LL and JY provided helpful guidance and suggestions, and PL supervised all of the study. All the authors read and approved the final manuscript.

Competing Interests

The authors declare that they have no competing interests.

Publisher's Note

Received: 29 October 2017 Accepted: 26 February 2018
Published online: 07 March 2018

References

1. Wu J, Agrawal M, Becerril HA, Bao Z, Liu Z, Chen Y, Peumans P (2010) Organic light-emitting diodes on solution-processed graphene transparent electrodes. ACS Nano 4:43–48

2. Liu P, Zeng BQ, Wang YX, Wang JH (2017) Transparent conductive nanowires thin films: preparation methods and applications in optoelectronic devices. Mater Rev 31(7):6–18
3. Yang J, Tang Q, Meng Q, Zhang Z, Li J, He B, Yang PJ (2017) Photoelectric conversion beyond sunny days: all-weather carbon quantum dot solar cells. J Mater Chem A 5:2143–2150
4. Wang C, Chen N, Liu YW, Zhao L, Xue DP, Du JH, Guo W, Wang L (2016) Influence factors of high thickness ITO residual in TFT process. Chin J Liq Crys Disp 31:276–282
5. Diao JJ, An LB, Chang CR (2016) Progress on the application of carbon nanotubes in typical micro and nano electronic devices. Chin J Liq Crys Disp 31:149–156
6. Yu P, Wu J, Liu S, Xiong J, Jagadish C, Wang ZM (2016) Design and fabrication of silicon nanowires towards efficient solar cell. Nano Today 11:704–737
7. Lin F, Zhu Z, Zhou X, Qiu W, Niu C, Hu J, Dahal K, Wang Y, Zhao Z, Ren Z, Litvinov D, Liu Z, Wang ZM, Bao J (2017) Orientation control of graphene flakes by magnetic field: broad device applications of macroscopically aligned graphene. Adv Mater 29:1604453
8. Ye S, Rathmell AR, Chen Z, Stewart IE, Wiley BJ (2014) Metal nanowire networks: the next generation of transparent conductors. Adv Mater 26:6670
9. Gordon RG (2000) Criteria for choosing transparent conductors. MRS bulletin 25(08):52–57
10. Leterrier Y, Médico L, Demarco FJ, Manson AE, Betz U, Escola MF, Olsson MK, Atamny F (2004) Mechanical integrity of transparent conductive oxide films for flexible polymer-based displays. Thin Solid Films 460:156–166
11. Celle C, Mayousse C, Moreau E, Basti H, Carella A, Simonato JP (2012) Highly flexible transparent film heaters based on random networks of silver nanowires. Nano Res 5:427–433
12. Mayousse C, Celle C, Moreau E, Mainguet JF, Carella A, Simonato JP (2013) Improvements in purification of silver nanowires by decantation and fabrication of flexible transparent electrodes. Application to capacitive touch sensors. Nanotechnology 24:215501
13. Hu L, Kim HS, Lee J, Peumans P, Cui Y (2010) Scalable coating and properties of transparent, flexible, silver nanowires electrodes. ACS Nano 4:2955–2963
14. Lee J, Lee I, Kim TS, Lee JY (2013) Efficient welding of silver nanowire networks without post-processing. Small 9:2887–2894
15. Liu CH, Yu X (2011) Silver nanowire-based transparent, flexible, and conductive thin film. Nanoscale Res Lett 6:75
16. Coskun S, Selen AE, Unalan HE (2013) Optimization of silver nanowire networks for polymer light emitting diode electrodes. Nanotechnology 24:125202
17. Mehra S, Christoforo MG, Peumans P, Salleo A (2013) Solution processed zinc oxide nanopyramid/silver nanowire transparent network films with highly tunable light scattering properties. Nanoscale 5:4400–4403
18. Khaligh HH, Goldthorpe IA (2013) Failure of silver nanowire transparent electrodes under current flow. Nanoscale Res Lett 8:235
19. Liang J, Li L, Niu X, Yu Z, Pei Q (2013) Elastomeric polymer light-emitting devices and displays. Nature Photonics 7:817–824
20. Mayousse C, Celle C, Carella A, Simonato JP (2014) Synthesis and purification of long copper nanowires. Application to high performance flexible transparent electrodes with and without PEDOT:PSS. Nano Research 7:315–324
21. Choi H, Park SH (2004) Seedless growth of free-standing copper nanowires by chemical vapor deposition. J Am Chem Soc 126:6248–6249
22. Zhang L, Yin J, Yu W, Wang M, Xie H (2017) Great thermal conductivity enhancement of silicone composite with ultra-long copper nanowires. Nanoscale Res Lett 12:462
23. Gao T, Meng G, Wang Y, Sun S, Zhang L (2002) Electrochemical synthesis of copper nanowires. J Phys: Condens Mat 14:355
24. Molares MET, Buschmann V, Dobrev D, Neumann R, Scholz R, Schuchert IU, Vetter J (2001) Single-crystalline copper nanowires produced by electrochemical deposition in polymeric ion track membranes. Adv Mater 13:62–65
25. Chang Y, Lye ML, Zeng HC (2005) Large-scale synthesis of high-quality ultralong copper nanowires. Langmuir 21:3746–3748
26. He X, He R, Liu AL, Chen X, Zhao Z, Feng S, Chen N, Zhang M (2014) A highly conductive, flexible, transparent composite electrode based on the lamination of silver nanowires and polyvinyl alcohol. J Mater Chem C 2:9737
27. Zhang X, Zhang D, Ni X, Zheng H (2006) One-step preparation of copper nanorods with rectangular cross sections. Solid State Commun 139:412–414
28. Wang W, Li G, Zhang Z (2007) A facile templateless, surfactantless hydrothermal route to ultralong copper submicron wires. J Cryst Growth 299:158–164
29. Shi Y, Li H, Chen L, Huang X (2005) Obtaining ultra-long copper nanowires via a hydrothermal process. Sci Technol Adv Mater 6:761–765
30. Mohl M, Pusztai P, Kukovecz A, Konya Z, Kukkola J, Kordas K (2010) Low-temperature large-scale synthesis and electrical testing of ultralong copper nanowires. Langmuir 26:16496–16502
31. Aziz A, Zhang T, Lin YH, Daneshvar F, Sue HJ, Welland ME (2017) 1D copper nanowires for flexible printable electronics and high ampacity wires. Nanoscale 9:13104–13111
32. Kim H, Choi SH, Kim M, Park JU, Bae J, Park J (2017) Seed-mediated synthesis of ultra-long copper nanowires and their application as transparent conducting electrodes. Applied Surface Science 422:731–737
33. Rathmell AR, Wiley BJ (2011) The synthesis and coating of long, thin copper nanowires to make flexible, transparent conducting films on plastic substrates. Adv Mater 23:4798–4803
34. Ye S, Rathmell AR, Stewart IE, Ha YC, Chen Z, Wiley BJ (2014) A rapid synthesis of high aspect ratio copper nanowires for high-performance transparent conducting films. Chem Commun 50:2562–2564
35. Chu HC, Chang YC, Lin Y, Chang SH, Chang WC, Li GA, Tuan HY (2016) Spray-deposited large-area copper nanowire transparent conductive electrodes and their uses for touch screen applications. ACS Appl Mater Interfaces 8:13009–13017
36. Zhu Y, Sun Z, Yan Z, Jin Z, Tour JM (2011) Rational design of hybrid graphene films for high-performance transparent electrodes. Acs Nano 5:6472–6479
37. Wu J, Zang J, Rathmell AR, Zhao X, Wiley BJ (2013) Reversible sliding in networks of nanowires. Nano Lett 13:2381–2386
38. Won Y, Kim A, Yang W, Jeong S, Moon J (2014) A highly stretchable, helical copper nanowire conductor exhibiting a stretchability of 700%. NPG Asia Materials 6(9):e132
39. Bergin SM, Chen YH, Rathmell AR, Charbonneau P, Li ZY, Wiley BJ (2012) The effect of nanowire length and diameter on the properties of transparent, conducting nanowire films. Nanoscale 4:1996–2004
40. Araki T, Jiu JT, Nogi M, Koga H, Nagao S, Sugahara T, Suganuma K (2014) Low haze transparent electrodes andhighly conducting air dried films with ultra-long silver nanowires synthesized by one-step polyol method. Nano Res 7:236–245
41. Jiu J, Araki T, Wang J, Nogi M, Sugahara T, Nagao S, Koga H, Suganuma K, Nakazawa E, Hara M, Uchida H, Shinozaki K (2014) Facile synthesis of very-long silver nanowires for transparent electrodes. J Mater Chem A 2:6326–6330